# Spider Monkey Optimization Based Fuzzy-2D-PID Controller for Load Frequency Control in Two-Area Multi Source Interconnected Power System

Debasis Tripathy
*Department of Electrical Engineering*
*NIT Silchar*
Assam,India
debasis.2404@gmail.com

Binod Kumar Sahu
*Department of Electrical Engineerin*
*Siksha 'O' Anusandhan University*
Bhubaneswar, India
binoditer@gmail.com

Bhaskar Patnaik
*Department of Electrical Engineering*
*R C E T, Bhilai*
Chhattisgarh, India
bhaskar7310@gmail.com

N.B. Dev Choudhury
*Department of Electrical Engineering*
*NIT Silchar*
Assam,India
nalinbdc@yahoo.com

***Abstract*** **- This paper presents a novel fuzzy logic based Two Degree of Freedom Proportional, Integral and Derivative controller (F2DPID) for load frequency control (LFC) in an interconnected two area multi-source power system. Spider Monkey Optimization (SMO) algorithm is used to optimize the controller parameters. Superiority of the proposed controller in terms of dynamic performances is established by comparing the results with conventional PID, two degree of freedom PID and fuzzy logic based PID controller. Initially, the study is carried out by considering the power system without any nonlinearity and then the study is extended by including nonlinearities like Governor Dead Band (GDB) and Generation Rate Constraint (GRC) in the same power system. The result is analyzed in terms of various time domain specifications such as settling time, peak undershoot, and peak overshoot of frequency and tie-line power deviations for Step Load Perturbation (SLP) of 1% in area-1.**

***Index Terms - Fuzzy-2D- PID controller (F2DPID), Load frequency control (LFC), Spider Monkey Optimization (SMO).***

## I. Introduction

In present scenario different areas of power system are interconnected together to improve the efficiency and reliability, which makes the system highly non-linear and complex in nature. The different area of interconnected power systems should operate at their nominal frequency for synchronism. The active power generation must be equal with active power demand and losses, so any mismatch between them due to the small disturbances in load can cause the deviation in system frequency and tie-line power flow in an interconnected power system. Control and exchange of power produced by different generating units to maintain frequency and tie-line power flows between different control areas at their nominal values are the main objective of load frequency control (LFC) [1]. It is noticeable from the literature that over the world many researchers have reported several techniques to retain the system frequency and tie line power exchange within specified limits during normal operation and also due to small step perturbations.

Initially, in 1956, Chon [2] projected the concept of AGC. Elgard et al. [3] in 1970 introduced the concept of modern optimal controller for AGC of an interconnected power system. Ghosal [4, 5] applied Particle Swarm Optimization (PSO), Genetic Algorithm (GA) and GA-SA algorithms to get optimal gains of fuzzy based PID controller for LFC. Nanda et al. [6] introduced Bacterial Foraging Optimization (BFO) algorithm to tune the parameters of controller for Automatic Generation Control (AGC) of multi-area power system. Khuntia et al. [7] proposed Artificial Neuro-Fuzzy Inference System (ANFIS) approach for AGC in multi-area power system. Saikia et al. [8] used BFO based fuzzy-IDD controller for analyzing the frequency stability in multi area thermal-hydro power system. Dash et al. [9] compared the performance of Cuckoo Search based different two degree of freedom (2DOF) controller for AGC of a multi area thermal power system. The parameters of 2DOF controller are optimized using Fire-Fly Algorithm proposed by Debbarma et al. [10], for AGC of multi area thermal system. Sahu et al. [11] proposed a Hybrid Differential Evolution (DE)-PSO fuzzy-PID controller for analyzing the dynamic performance of AGC system of a two and a three-area reheat thermal system. Mohanty et al. [12] projected DE algorithm based PI controller for AGC of two-area, multi-source considering nonlinearity. Sahu et al. [13] proposed Teaching Learning Based Optimization (TLBO) algorithm initially for two area thermal system and then, extended to multi-area with diverse energy sources including nonlinearity. Hybrid Local Unimodal Sampling (LUS)-TLBO based fuzzy-PID controller is introduced by Sahu et al. [14] for LFC of two area multi-source interconnected system by incorporating HVDC link. Soni et al. [15] proposed hybrid Grey Wolf-Pattern search

978-1-5386-4581-9/18/$31.00 ©2018 IEEE

(hGWO-PS) algorithm to get optimal value of 2DOF controller gains of thermal power system for AGC in an interconnected.

The literature study concludes that, as per the author's knowledge previously no author reported about fuzzy two degree of freedom (F2DPID) controller to solve LFC related problems. As high efficient optimization technique is always welcome to tune the controller parameters for achieving better system performance, a new population based intelligent technique known as Spider Monkey Optimization (SMO) algorithm developed and introduced by Bansal (2014) has been considered in this article. Some advantages of the proposed algorithm are:

- It perfectly balances both exploration and exploitation.
- It helps in avoiding stagnation and premature convergence as it uses four parameters namely perturbation rate (*Pr*), maximum number of groups (*MG*), global leader limit ($GL_{lmt}$), and local leader limit ($LL_{lmt}$).

This work is focused to introduce SMO algorithm based F2DPID controller for LFC of an interconnected two area power system. To establish the superiority for proposed controller over other controllers, the dynamic performance indices of the proposed system like overshoots, undershoots and settling times has been compared for two different cases i.e. system without having non linearity and system with nonlinearities like GDB and GRC to make the power system more realistic.

## II. System Model

Figure 1 shows the block diagram representation of a two equal area interconnected power system. Area-1 consists of thermal and wind generator with an area participation factor (apf) of 0.9 and 0.1 respectively but area-2 is combination of a hydro and a diesel unit with apf of 0.9 and 0.1respectively. Rating of each area is 2000 MW having nominal load of 1000 MW. Normally, wind and diesel generating units are incorporated with thermal and hydro generating units to supply the peak load demand.

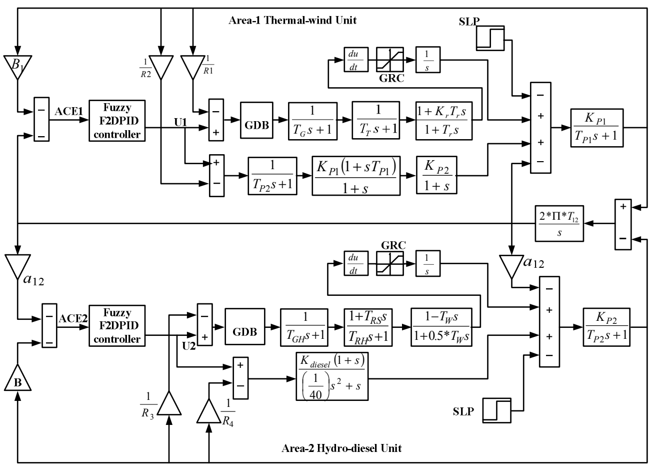


Fig.1. Transfer function model of the proposed power system

Presence of Governor dead band (GDB) nonlinearity in power system causes oscillation in system dynamics. GDB is the net amount of a continual speed change within which there is no change in valve position. In the present work dead band of 0.05% for the thermal system and 0.02% for hydro system is considered [12, 13]. In a power system power generation can change only at a specified maximum rate known as Generation Rate Constraint (GRC). In the current study considered GRC of 3% per min for thermal unit, 270% per minute and 360% per minute for raising and lowering generation in hydro unit respectively. [12, 13].SMO optimized F2DPID controller is implemented in both the areas as a secondary controller for controlling the tie-line power flow and frequency.

Input signals to the fuzzy controller are Area Control Errors (ACEs) of the respective area (which is the linear combination of frequency and tie-line power) and its first derivative (ΔACE), where as $U_1$, $U_2$ are the output signal. When the system is subjected to a sudden small perturbation, ACEs act as actuating signals for respective controllers. In Fig.1, $B_1$ and $B_2$ are the frequency bias factors, $R_1$ and $R_2$ are speed regulation of governors, $\Delta f_1$ and $\Delta f_2$ are the deviations in frequencies, $\Delta P_{12}$ and $\Delta P_{21}$ are tie-line power flow change between the areas, $K_{P1}$ and $K_{P2}$ are gains of power system, $T_{P1}$ and $T_{P2}$ are power system time constants of area-1 and area-2 respectively. $T_{12}$ is the synchronizing torque coefficient. Parameters used for different generating units in the proposed model under study are provided in Appendix.

## III. Controller Structure

Degree of freedom can be defined by the number of closed-loop transfer functions which can be adjusted independently. 2DOF controller shows superior performance over the single degree of freedom as it has two closed loop transfer functions [9, 10, 15,]. 2DOF controller determines a weighted difference between reference signal R(s) which is the output of fuzzy-PD section of proposed controller and feedback signal (measured system output) for each of the proportional, integral and derivative action as per the specified set point weights. Controller output is the sum of outputs of individual actions on their corresponding difference signals, where each action is weighted as per the selected gain parameters [15].

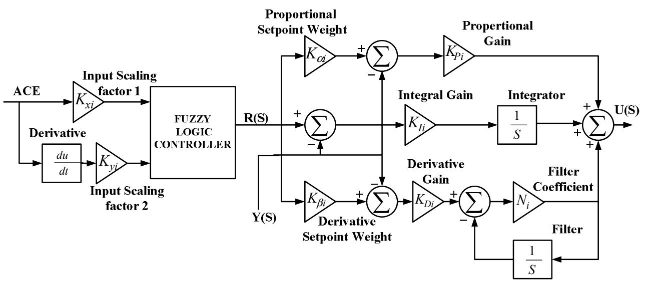


Fig. 2. Block diagram representation of the fuzzy-2D-PID Controller

General structure of a F2DPID controller is shown in Fig.2. It is a cascade connection of fuzzy-PD and conventional 2DPID controller. The input gains of proposed controller are

$K_{Xi}$, $K_{Yi}$ and $K_{Pi}$, $K_{Ii}$, $K_{Di}$,$K_{\alpha i}$,$K_{\beta i}$ are the output gains, where first three are for proportional, integral, derivative gains and last two are set point weight with suffix $i$=1, 2 representing area-1 and 2 respectively. As gains of the F2DPID controller are the main cause to improve the system performance, so these must be designed optimally. ACE and derivative of ACE (ΔACE) are the two inputs for the proposed controller.

$$(ACE_i) = B_i \times (\Delta f)_i + (\Delta P_{tie-12})_i \quad (1)$$

where, i=1, 2 for area-1 and area-2 respectively

Triangular fuzzy membership functions are used with five linguistic variables such as: Big Negative (BN), Small Negative (SN), Zero Error (ZE), Small Positive (SP) and Big Positive (BP) for both the inputs and the output [14]. Mamdani fuzzy inference engine and centre of gravity method of defuzzification is selected for this paper for simplicity. Structure of membership function for both the inputs and output is shown in Fig.3 [15]. Two-dimensional rule base for error & derivative of error is depicted in Table I [11].

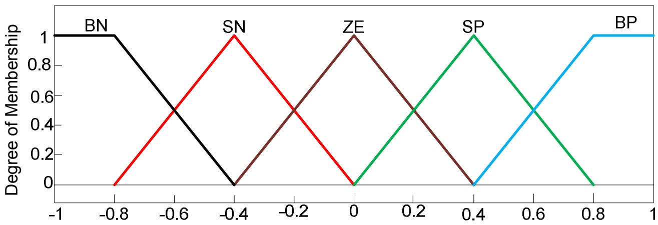


Fig. 3. Structure of triangular membership function

Table I. Rule base for error,change in error and output of fuzzy controller

| ACE | ΔACE | | | | |
|---|---|---|---|---|---|
| | BN | SN | ZE | SP | BP |
| BN | BN | BN | SN | SN | ZE |
| SN | BN | SN | SN | ZE | SP |
| ZE | SN | SN | ZE | SP | SP |
| SP | SN | ZE | SP | SP | BP |
| BP | ZE | SP | SP | BP | BP |

Objective function chosen for the present study is Integral Time Absolute Error (ITAE), as it is the time multiplication of absolute value of frequency and tie-line power deviations, it is better than other objective functions in the field of LFC [11]

$$J = ITAE = \int_0^{t_{sim}} \left[ |\Delta f_1| + |\Delta f_2| + |\Delta P_{tie-12}| \right] \cdot t \cdot dt \quad (2)$$

where, $t_{sim}$ is the simulation time and $\Delta P_{tie-12}$ is the tie-line power exchange between area-1 & area-2.

## IV. Spider Monkey Optimization Algorithm

Spider Monkey Optimization (SMO) algorithm is a meta-heuristic nature-inspired population based algorithm. This algorithm was proposed and introduced by Bansal [16] in 2014. Social animals like spider monkeys dwell in a core group with 40–50 individuals. A female member of the core group known as global leader leads the group and responsible to find enough food for group members. In case, she is unable to find enough food for the group members then, she divides the core group into smaller groups known as local groups. Local groups or sub groups again led by a female member with a size of 3-6 individuals. Then the sub groups start foraging in different direction during the day time and finally at the end of the day they recombine the group to share foods and other experiences. The strategy adopted by these monkeys for foraging foods falls them into a class of fission-fusion social structure (FFSS) animals. The way in which these social animals are foraging foods for their groups inspired the author to simulate and develop the algorithm. Perturbation rate ($pr$), maximum number of groups ($MG$), local leader limit ($LL_{lim}$), and global leader limit ($GL_{lim}$) are the four control parameter of algorithm which takes care of the balance between both exploration and exploitation of search space and also about premature convergence & stagnation issues. The details of algorithm and pseudocode are discussed in [16, 17]. Different phases of SMO algorithms are briefly deliberated next.

### *A. Initialization of the population*

In the initialization phase, SMO generates a uniformly distributed population with dimension $[n \times d]$, where '$n$' is number of monkeys or population size and 'd' is the number of control variables which are to be optimized. Each monkey in the population is initialized by equation (3).

$$M_{xy} = M_{\min y} + (M_{\max y} - M_{\min y}) \times U(0,1) \quad (3)$$

where, $M_{maxy}$ and $M_{miny}$ are the upper and lower bound of $x^{th}$ *monkey* in $y^{th}$ direction and $U$ (0, 1) is a random number which distributed uniformly within a range [0, 1].

### *B. Local Leader Phase (LLP)*

This phase is mainly meant for exploring the search space, where individual monkey update their current position based on the experience of local leader and local group members. Equation (4) is used to update position $x^{th}$ monkey (which belongs to $p^{th}$ local group) corresponding to new position. Perturbation rate (pr) decides the amount of change in current position so it has to be chosen carefully.

$$M_{newxy} = M_{xy} + (LL_{py} - M_{xy}) \times U(0,1) + (M_{qy} - M_{xy}) \times U(-1,1) \quad (4)$$

where, $M_{xy}$ is the $y^{th}$ dimension of the $x^{th}$ monkey, $LL_{py}$ represents the $y^{th}$ dimension of $p^{th}$ local group leader position. $M_{qy}$ is the $y^{th}$ dimension of $q^{th}$ monkey which is chosen randomly within $p^{th}$ group such that q≠x, U (-1, 1) is a random number in the range [-1, 1].

### *C. Global Leader Phase (GLP)*

Global leader phase is mainly used for exploitation, where all the monkeys update respective positions with the experience of global leader and local group members. Equation (5) is used to update the position.

$$M_{newxy} = M_{xy} + (GL_{xy} - M_{xy}) \times U(0,1) + (M_{qy} - M_{xy}) \times U(-1,1) \quad (5)$$

where, $GL_y$ represents the global leader position in $y^{th}$ dimension. With equation (6), the position of $x^{th}$ monkey get updated based on a factor known as probabilities ($prb_x$).

$$prb_x = 0.1 + \left( \frac{fit_x}{\max\_fit} \right) \times 0.9 \tag{6}$$

where, $fit_x$ the fitness is value of $x^{th}$ monkey and *max_fit* is the maximum fitness in the group. In this way, monkey who is having better fitness get more chances to update its position.

### *D. Local Leader Learning (LLL) phase*

In this phase, local leader position gets updated using greedy selection (i.e. position of monkey with best fitness in that group). If local leader position is not updated then, local limit count is incremented by unity.

### *E. Global Leader Learning (GLL) phase*

In this phase, greedy selection is used for updating the global leader position of. Further new position is compared with old position of global leader, if it is not updated then the global limit count is incremented by unity.

### *F. Local Leader Decision (LLD) phase*

In this phase, position of local leader if not updated for a pre-specified number of trials (= local leader limit) then each and every members of that group must be reinitialized. Initialization of individual member of that group can either be generated randomly or generated by collecting information from local leader and global leader using equation (7).

$$\begin{aligned} M_{newxy} &= M_{xy} + \left(GL_y - M_{xy}\right) \times U(0,1) \\ &+ \left(M_{xy} - LL_{py}\right) \times U(0,1) \end{aligned} \tag{7}$$

Above equation shows that, the updated dimension of monkey gets attracted towards global leader and repelled from local leader.

### *G. Global Leader Decision (GLD) phase*

In this phase, if global leader position remains unchanged for predefined number of trials (= global leader limit) then global leader recombine whole population into a single group, again starts dividing into number of small groups preliminary with two, then three, and so on.

## V. Result Analysis

The model under study is developed and simulated in MATLAB (R2010a) /SIMULINK environment using an Intel, core i3 processor of 2.4 GHz and 2 GB RAM computer. The objective function is calculated and a separate program for SMO algorithm is written in.mfile to optimize the controller parameters considering a 1% step load change in area-1. The following parameters are chosen for SMO algorithm: population size NP = 50; Maximum number of iteration = 100; global leader limit ($GL_{lim}$) = 25, local leader limit ($LL_{lim}$) = 50, maximum number of group = 10, perturbation rate increases linearly from 0.1 to 1 with time. The optimization was repeated 30 times and the best solution out of 30 runs is chosen as optimal parameters for controller. The optimal solutions obtained for controller gains and objective functions (ITAE) for different controllers are shown in Table II.

### *A. Without considering nonlinearity*

The system considered for the study is a two area multi source with 2000 MW each and a nominal loading of 1000 MW (area-1 having thermal and wind generating units and area-2 consists of hydro & diesel generating units). Dynamic performance of SMO optimized F2DPID controller is compared with other controllers such as PID, 2DPID and FPID. From Table II, it is interpreted that the objective function (J) obtained for proposed F2DPID controller is minimum (ITAE=0.0148) over others.

So, it can be concluded that for same optimization technique & objective function (ITAE), F2DPID controller performs better in terms of transient performance indexes like overshoot, undershoot and settling time as compared to other controllers. Table III, depicts the values of these performance indexes for different controllers and Figs. 4(a)-4(c) shows the comparison of simulation results for frequency deviations in area-1& area-2 and tie-line power flow deviation respectively. Analysis of the dynamic responses clearly reveals that there is a significant improvement in oscillation (i.e. oscillation dies out) with SMO based F2DPID controller.

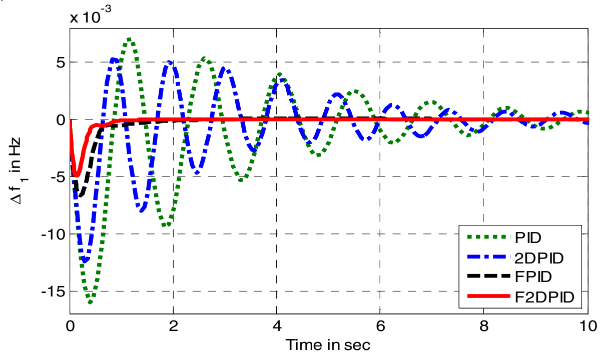


Fig. 4(a). Frequency deviation in Area-1 without nonlinearity

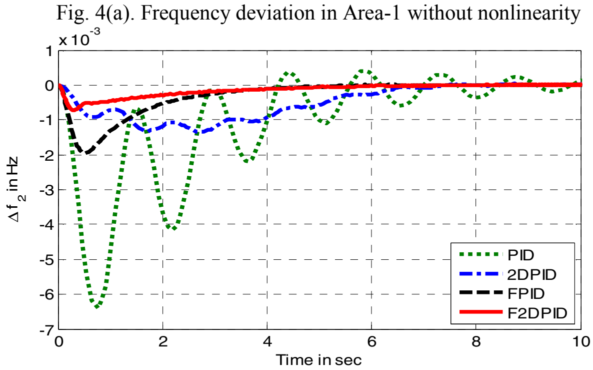


Fig. 4(b). Frequency deviation in Area-2 without nonlinearity

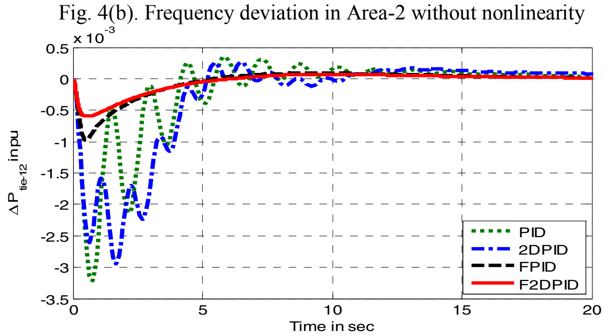


Fig. 4(c). Tie-Line power deviation without nonlinearity

Table II. Optimum values of the controller gains with and without nonlinearity

| Controller Gains | Without Non- linearity | | | | With Non-Linearity | | | |
|---|---|---|---|---|---|---|---|---|
| | PID | 2DPID | FPID | F2DPID | PID | 2DPID | FPID | F2DPID |
| $K_{X1}$ | --- | --- | 1.9930 | 1.9997 | --- | --- | 1.9999 | 1.9985 |
| $K_{Y1}$ | --- | --- | 0.6674 | 1.5882 | --- | --- | 0.6433 | 0.8845 |
| $K_{\alpha1}$ | --- | 0.1519 | --- | 0.9999 | --- | 1.4625 | --- | 0.2461 |
| $K_{\beta1}$ | --- | 0.0001 | --- | 0.5280 | --- | 0.0003 | --- | 1.4080 |
| $K_{P1}$ | 0,0001 | 0.0127 | 1.2892 | 1.1066 | 0.0050 | 0.0297 | 1.4132 | 0.1814 |
| $K_{I1}$ | 1.2102 | 0.7609 | 1.7900 | 1.9966 | 1.6630 | 1.1997 | 1.9999 | 1.9862 |
| $K_{D1}$ | 1.1964 | 1.4693 | 0.5379 | 0.0561 | 1.5014 | 1.3682 | 0.4990 | 1.3874 |
| $K_{X2}$ | --- | --- | 0.3490 | 1.7388 | --- | --- | 0.4744 | 0.8881 |
| $K_{Y2}$ | --- | --- | 0.3790 | 1.0373 | --- | --- | 0.0473 | 0.6924 |
| $K_{\alpha2}$ | --- | 0.0001 | --- | 0.5354 | --- | 1.7027 | --- | 1.7992 |
| $K_{\beta2}$ | --- | 0.7525 | --- | 0.1775 | --- | 1.7629 | --- | 0.1136 |
| $K_{P2}$ | 1.9250 | 1.9999 | 1.9999 | 1.8258 | 0.9698 | 1.0169 | 1.9999 | 0.7745 |
| $K_{I2}$ | 0.7619 | 1.9205 | 0.4466 | 0.1937 | 1.5186 | 1.1620 | 0.0001 | 1.5816 |
| $K_{D2}$ | 1.9145 | 1.5239 | 0.7309 | 0.2095 | 1.9999 | 1.3781 | 1.9999 | 0.3835 |
| **ITAE (J)** | **0.1579** | **0.1392** | **0.0184** | **0.0148** | **0.3036** | **0.1852** | **0.0361** | **0.0288** |

Table III. $U_{SH}$, $O_{SH}$ & $T_S$ of different controller with and without nonlinearity

| Transient Parameters | | Without Non- linearity | | | | With Non-Linearity | | | |
|---|---|---|---|---|---|---|---|---|---|
| | | PID | 2DPID | FPID | F2DPID | PID | 2DPID | FPID | F2DPID |
| $\Delta f_1$ | $U_{SH}\times10^{-3}$ in Hz | -16.0187 | -12.4018 | -6.6341 | **-4.9558** | -16.7668 | -13.7967 | -8.8373 | **-6.2090** |
| | $O_{SH}\times10^{-3}$ in Hz | 7.0221 | 5.3214 | 0.1109 | **0.0565** | 7.9801 | 7.4084 | 0.3471 | **0.276** |
| | $T_S$ in sec | 17.2214 | 13.8093 | 1.7245 | **0.8548** | 19.1712 | 14.3542 | 5.4317 | **2.1397** |
| $\Delta f_2$ | $U_{SH}\times10^{-3}$ in Hz | -6.4074 | -1.3457 | -1.9621 | **-0.7221** | -6.8624 | -2.6981 | -3.2626 | **-1.4161** |
| | $O_{SH}\times10^{-3}$ in Hz | 0.4067 | 0.1173 | 0.0226 | **0.0221** | **0.0065** | 0.0126 | 0.0350 | 0.0299 |
| | $T_S$ in sec | 14.7461 | 6.1691 | 3.2652 | **2.7975** | 17.9868 | 12.2664 | 6.945 | **5.8403** |
| $\Delta P_{tie-12}$ | $U_{SH}\times10^{-3}$ in p.u | -3.2149 | -2.9408 | -0.9804 | **-0.5866** | -3.5410 | -2.9209 | -1.6345 | **-1.131** |
| | $O_{SH}\times10^{-3}$ in p.u | 0.3528 | 0.2605 | 0.0902 | **0.0665** | 0.1829 | **0.00** | 0.0149 | 0.0195 |
| | $T_S$ in sec | 8.946 | 6.6572 | 3.2204 | **3.1625** | 11.9092 | 14.7410 | 7.3048 | **6.579** |

### *B. With GRC & GDB nonlinearity.*

To make the study more realistic for LFC problem, it is essential to consider the some inherent requirement and basic physical constraints in the model. Reheat turbine (As most of the thermal generating units are employed with reheat turbine) Boiler Dynamics (BD) Generation Rate Constraint (GRC), Governor Dead Band (GBD) are the major constraints that affects the power systems' performance. To get accurate insight, the study is extended further by considering the effect of reheat turbine, GRC and GBD.

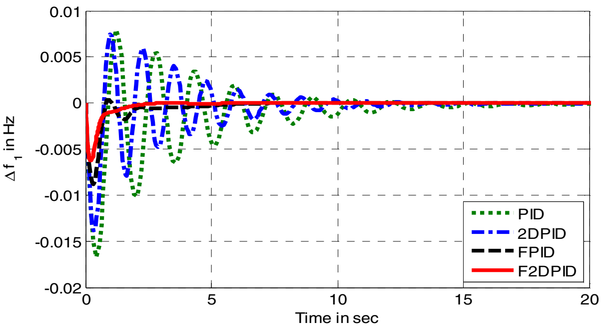


Fig. 5(a). Frequency deviation in Area-1with Nonlinearity

Optimal controller gains obtained for AGC of the power system with nonlinearities are depicted in Table II. Undershoot, overshoot and settling time (0.0002 band) of tie-line power and frequency deviations are given in Table III. Figure 5(a)-5(b) represent frequency deviation in area-1, in area-2 and tie-line power deviation respectively. It is clear from Table III and Fig. 5(a)-5(b) that the proposed F2DPID controller is more effective to reduce oscillation and also gives best system performance with minimum values of settling times, peak undershoot and peak overshoots in frequency deviations in both the areas and tie-line power flow between them.

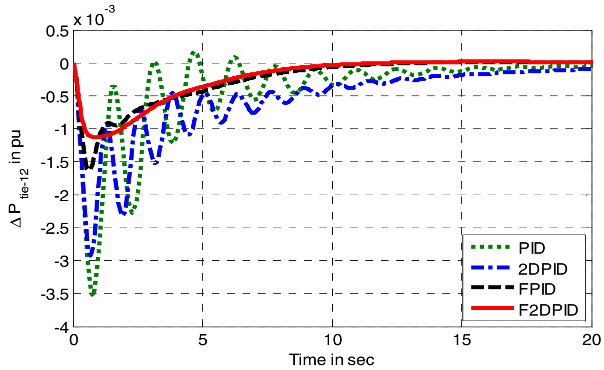


Fig. 5(b). Tie-Line power deviation with Nonlinearity

## VI. CONCLUSION

The objective of present study is to introduce a novel F2DPID controller as a secondary controller for LFC in an interconnected multi source power system. A two area equal rating power system (i.e. area-1 consisting of thermal & wind generating units and hydro & diesel generating units are in area-2) is considered and a nature inspired population based meta-heuristic SMO algorithm with ITAE as objective function is employed for optimizing the controller parameters. To establish the superiority of proposed SMO based F2DPID controller over other controllers two different cases have been considered such as: (i) absence of nonlinearity in the system and (ii) presence of GRC & GDB nonlinearity in the system to make it more realistic. It is observed from the results that the performance of proposed controller is superior in terms of settling time, undershoot and peak overshoot as well as the oscillation in the system performance dies out significantly for the same system due to a step load perturbation (SLP) of 1 % in area-1.

## APPENDIX [13,14]

f = 60 Hz; $R_1 = R_2 = R_3 = R_4 = 2.4$Hz/p.u.; $T_{PS1} = T_{PS2} = 20$ s; $K_{PS1} = K_{PS2} = 120$ Hz/p.u.MW; $B_1 = B_2 = 0.425$ p.u. MW/Hz.
Thermal Unit: $T_G = 0.08$ s; $T_T = 0.3$ s; $K_r = 0.333$; $T_r = 10$ s.
Hydro Unit : $T_{GH} = 48.7$ s; $T_{RS} = 0.513$ s; $T_{RH} = 10$ s; $T_W = 1$.
Wind Unit : $T_{P1} = 6$; $T_{P2} = 0.041$; $K_{P1} = 1.25$; $K_{P2} = 1.4$.
Diesel Unit : $K_{diesel} = 16.5$.

## ACKNOWLEDGEMENT

Authors extend their hearty thanks to EE department and TEQIP-III, NIT Silchar, for support and funding for this work..

## REFERENCES

[1] P. Kundur, “Power system stability and control,” 4th reprint. Tata McGraw-Hill, New Delhi, 200, pp. 581-623.
[2] N. Cohn, "Some aspects of tie-line bias control on interconnected power systems," *Transactions of the American Institute of Electrical Engineers. Part III: Power Apparatus and Systems,* vol.75 (3), 1956, pp. 1415-1436.
[3] O. I. Elgerd and C. E. Fosha, "Optimum megawatt-frequency control of multi area electric energy systems," IEEE Transactions on Power Apparatus and Systems, vol.4, 1970, pp. 556-563.
[4] S. P. Ghoshal, "Optimizations of PID gains by particle swarm optimizations in fuzzy based automatic generation control," Electric Power Systems Research, vol. 72(3), 2004, pp. 203-212.
[5] S. P. Ghoshal, "Application of GA/GA-SA based fuzzy automatic generation control of a multi-area thermal generating system," Electric Power Systems Research, vol.70 (2), 2004, pp. 115-127.
[6] J. Nanda, S. Mishra, and L. C. Saikia, "Maiden application of bacterial foraging-based optimization technique in multiarea automatic generation control," IEEE Transactions on Power Systems, vol. 24(2), 2009, pp. 602-609.
[7] S. R. Khuntia and S. Panda, "Simulation study for automatic generation control of a multi-area power system by ANFIS approach," Applied Soft Computing, vol.12(1), 2012, pp. 333-341.
[8] L. C. Saikia, N. Sinha, and J. Nanda, "Maiden application of bacterial foraging based fuzzy IDD controller in AGC of a multi-area hydrothermal system," International Journal of Electrical Power & Energy Systems, vol. 45(1), 2013, pp. 98-106.
[9] P. Dash, L. C. Saikia, and N. Sinha, "Comparison of performances of several Cuckoo search algorithm based 2DOF controllers in AGC of multi-area thermal system," International Journal of Electrical Power & Energy Systems, vol. 55, 2014, pp. 429-436.
[10] S. Debbarma, L. C. Saikia, and N. Sinha, "Robust two-degree-of-freedom controller for automatic generation control of multi-area system," International Journal of Electrical Power & Energy Systems, vol. 63, 2014, pp. 878-886.
[11] B. K. Sahu, S. Pati, and S. Panda, "Hybrid differential evolution particle swarm optimisation optimised fuzzy proportional–integral derivative controller for automatic generation control of interconnected power system," IET Generation, Transmission & Distribution, vol. 8(11), 2014, pp. 1789-1800.
[12] B. Mohanty, S. Panda, and P. K. Hota, "Differential evolution algorithm based automatic generation control for interconnected power systems with non-linearity," Alexandria Engineering Journal, vol. 53(3), 2014, pp. 537-552.
[13] R. K. Sahu, G. T. C. Sekhar, and S. Panda, "Automatic generation control of multi-area power systems with diverse energy sources using teaching learning based optimization algorithm," Engineering Science and Technology, an International Journal, vol. 19(1), 2016, pp. 113-134.
[14] B. K. Sahu, T. K. Pati, J. R. Nayak, S. Panda, and S. K. Kar, "A novel hybrid LUS–TLBO optimized fuzzy-PID controller for load frequency control of multi-source power system," International Journal of Electrical Power & Energy Systems, vol. 74, 2016, pp. 58-69.
[15] V. Soni, G. Parmar, M. Kumar, and S. Panda, "Hybrid Grey Wolf Optimization-pattern search (hGWO-PS) optimized 2DOF-PID controllers for load frequency control (LFC) in interconnected thermal power plants," ICTACT Journal on Soft Computing, vol. 6(3), 2016, pp.244-1256.
[16] J. C. Bansal, H. Sharma, S. S. Jadon, and M. Clerc, "Spider monkey optimization algorithm for numerical optimization," Memetic Computing, vol. 6(1), 2014, pp. 31-47.
[17] K. Gupta, K. Deep, and J. C. Bansal, "Spider monkey optimization algorithm for constrained optimization problems," Soft Computing, vol. 21(23), 2017, pp. 6933-6962.